Impaired respiration discloses the physiological significance of state transitions in *Chlamydomonas*

Pierre Cardol[a], Jean Alric[b], Jacqueline Girard-Bascou[b], Fabrice Franck[c], Francis-André Wollman[b,1], and Giovanni Finazzi[b,1]

[a]Laboratoire de Génétique des Microorganismes et [c]Laboratoire de Photobiologie, Département des Sciences de la Vie, Université de Liège, B-4000 Liège, Belgique; and [b]Institut de Biologie Physico-Chimique, Unité Mixte de Recherche 7141, Centre National de la Recherche Scientifique and Université Pierre et Marie Curie-Paris 6, 75005, Paris, France

State transitions correspond to a major regulation process for photosynthesis, whereby chlorophyll protein complexes responsible for light harvesting migrate between photosystem II and photosystem I in response to changes in the redox poise of the intersystem electron carriers. Here we disclose their physiological significance in *Chlamydomonas reinhardtii* using a genetic approach. Using single and double mutants defective for state transitions and/or mitochondrial respiration, we show that photosynthetic growth, and therefore biomass production, critically depends on state transitions in respiratory-defective conditions. When extra ATP cannot be provided by respiration, enhanced photosystem I turnover elicited by transition to state 2 is required for photosynthetic activity. Concomitant impairment of state transitions and respiration decreases the overall yield of photosynthesis, ultimately leading to reduced fitness. We thus provide experimental evidence that the combined energetic contributions of state transitions and respiration are required for efficient carbon assimilation in this alga.

cyclic electron flow | photosynthesis | energetic metabolism

State transitions (ST) are a short-term photosynthetic acclimation process that controls the reversible association of the photosystem II (PSII) antenna protein complex (LHCII) with either PSII (in state 1) or photosystem I (PSI) (in state 2) (1–3). This process relies on the reversible LHCII phosphorylation involving the membrane-bound protein kinase Stt7-STN7, which recently has been identified in *Chlamydomonas reinhardtii* and *Arabidopsis thaliana* (4, 5). Phosphorylation changes lead to the migration of a fraction of the antenna between the PSII-enriched membrane domains and the PSI-enriched membrane domains within the thylakoids in plant and algal chloroplasts (3, 6).

STs first were observed in unicellular green algae and originally were described as a mechanism linking the redox poise of the intersystem electron carriers to changes in the absorption capacity of the photosystems (3). Reduction of the plastoquinone (PQ) pool upon increased PSII sensitization activates the kinase via the cytochrome b_6f complex (7). Conversely, upon increased PSI sensitization, PQH_2 oxidation inactivates the kinase. P_i-LHCII then is dephosphorylated by a phosphatase (3) whose biochemical nature and regulation remain elusive.

In plants, STs are of limited amplitude, involving ≈20% of LHCII (8). Their occurrence probably is not essential for plant survival, as suggested by the very limited effects on growth (4, 9–11) and on fitness (12) of mutations preventing STs in *Arabidopsis*. One of these mutants shows a marked phenotype only under a very particular regimen of fluctuating light (4). In *Chlamydomonas*, STs involve a larger fraction of PSII antenna than in plants, with ≈80% of PSII antennae being involved in this phenomenon (13), including monomeric LHCII (14). The very large redistribution of light-harvesting complexes with STs in this alga is difficult to reconcile with a role of merely balancing light absorption. Indeed, the huge decrease in PSII absorption (by a factor of ≈2) leads to unbalanced PSI and PSII absorption capacity in state 2 (15). This large energy redistribution between

the 2 photosystems largely favors PSI photochemistry at the expense of PSII in light-limiting conditions. Based on a number of experiments, it was concluded that STs in *Chlamydomonas* serve to change the ratio between linear and cyclic electron flow (CEF) around PSI (2). It thus came as a surprise that there was no specific growth defect in mutants lacking the STT7 kinase that controls STs in *Chlamydomonas* (16).

A tight interplay between respiratory activity and STs has been reported earlier in dark-adapted *Chlamydomonas*. This interplay was documented using inhibitors of mitochondrial respiration or by analysis of respiratory-deficient mutants (17, 18). In both cases, impaired respiration depleted intracellular ATP pools in the dark, stimulating glycolysis according to the Pasteur effect. Released reductants in the chloroplast stroma enhanced non-photochemical reduction of the PQ pool in the thylakoid membranes, favoring acclimation to state 2 in darkness. Subsequent illumination restored ATP cellular levels and allowed partial reoxidation of the PQ pool and transition to state 1. Based on these earlier observations, we decided to explore the possible role of STs on photosynthesis in *Chlamydomonas* in relationship to changes in respiratory efficiency. We used a genetic approach to compare photosynthetic efficiency in mutants impaired in respiration and/or in ST.

Results

The Absence of State Transitions in a Respiration-Defective Context Is Detrimental for Cell Growth in *Chlamydomonas*. We first assessed the possible interplay between STs and respiration during illumination by comparing growth of the ST-competent wild type and the ST-defective *stt7–9* mutant under photoautotrophic and mixotrophic conditions. As indicated by the growth on solid media (Fig. 1*A*) or by the doubling times in liquid cultures (Fig. 1*B*), there were no significant differences between the 2 strains (16), suggesting that STs are dispensable for biomass generation in these experimental conditions when both photosynthesis and respiration are fully active. Addition of myxothiazol, a known inhibitor of mitochondrial respiration, led to decreased growth in mixotrophic conditions in the 2 strains, consistent with the prominent role of respiration in acetate assimilation. Nevertheless, a larger effect was seen in *stt7–9* cells, suggesting a possible specific inhibitory effect in this strain. Consistent with this hypothesis, a marked contrast became apparent between the growth rates of the 2 strains when myxothiazol was added in photoautotrophic conditions. Myxothiazol drastically reduced growth in *stt7–9* cells (Fig. 1 *A* and *B*), but it had only a marginal
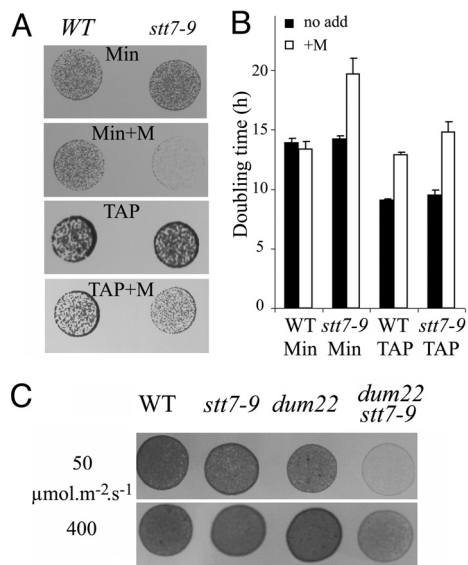
Fig. 1. Impact of inhibition of the mitochondrial respiratory chain on growth of ST-deficient strain. Cells were cultivated at 50 μmol photons m^{-2}s^{-1} in mixotrophic (TAP) or photoautotrophic (Min) conditions in the absence or presence (+M) of the mitochondrial respiratory inhibitor myxothiazol (5 μM). (A) Drops of cell suspensions ($\approx$0.01 nm A$_{750}$) were plated on solid media, and growth was estimated after 3 to 5 days. (B) Doubling time in liquid cultures. Error bars indicate standard deviation of the mean of 3 independent measurements. (C) The experimental procedure is the same as in A. Photoautotrophic (Min) conditions. Light intensity was either 50 or 400 μmol photons m^{-2}s^{-1}.

effect in wild-type cells, suggesting that efficient photosynthetic growth requires respiration in the absence of ST.

This observation prompted us to use a genetic approach to explore further the interplay between ST and respiration. We resorted to *Chlamydomonas* mutants defective in mitochondrial activity (*dums*) (19) to generate a double mutant impaired in both ST and mitochondrial respiration. To this end, we crossed the *dum22 mt^{-}* mitochondrial mutant (lacking both complex I and III activities) with the *stt7–9 mt^{+}* nuclear mutant devoid of ST because of the absence of the Stt7 kinase. We isolated 7 *dum22 stt7–9* clones defective in ST and in mitochondrial respiration (see Fig. S1 *A and B*, Table S1, and *SI Methods*). We then compared these clones with their parental strains for growth capacity in photoautotrophic and mixotrophic conditions (Fig. 1*C* and Fig. S1*C*). In line with the observations drawn from the use of respiration inhibitors, we found that the combined defects in respiration and ST led to a severe decrease in growth rates. We first ruled out the possibility that the growth defect could originate from increased photosensitivity. Indeed, *dum22 stt7–9* did not show further growth inhibition in phototrophic conditions when the light intensity was increased (Fig. 1*C*). In addition, no statistically significant differences in photosensitivity were seen when measuring changes in the photosynthetic efficiency (Fv/Fm) in wild-type, *stt7–9*, *dum22*, and *dum22 stt7–9* cells exposed to saturating light (Fig. S2). Thus, we concluded that some metabolic features of *dum22 stt7–9* limit growth rate in photoautotrophic conditions.

Functional Characteristics of *dum22 stt7–9*. To understand which factors limit the growth rate of *dum22 stt7–9* in photoautotrophic conditions, we further characterized its photosynthetic properties. Recent data have suggested that ST may contribute to long-term acclimation via the regulation of gene expression (9, 10). In particular, it has been suggested that ST may modulate the relative amounts of active PSI and PSII in plants acclimated
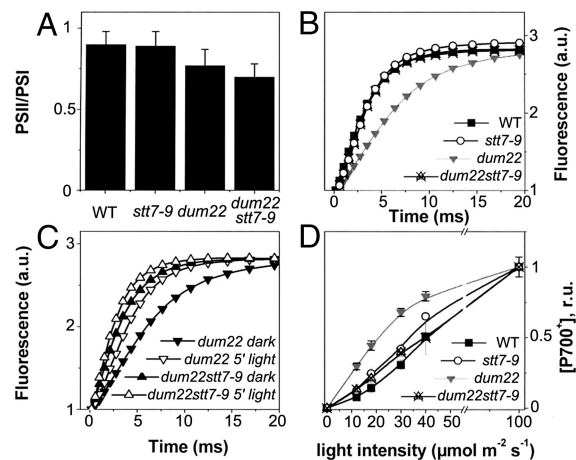
Fig. 2. Comparative analysis of the photosynthetic features of the *dum22 stt7–9* mutant (*A*) PSII/PSI ratios. Changes in the amplitude of the fast phase of the ECS signal (at 520–545 nm) upon excitation with a saturating laser flash in the presence or absence of PSII inhibitors DCMU (20 μM) and hydroxylamine (1 mM) were used to assess PSI and PSII stoichiometry. (*B*) Relative antenna size in PSII, as evaluated form fluorescence induction kinetics. Curves were normalized to the same value of variable fluorescence to allow a better comparison. Closed squares, wild type cells; open circles, *stt7–9* cells; downwards gray triangles, *dum22* cells; upwards crossed triangles, *dum22 stt7–9* mutants. (*C*) Effect of preillumination on PSII relative antenna size in *dum22* cells and *dum22 stt7–9* mutant cells. Solid symbols, dark adaptation for 20 min under strong agitation; open symbols, exposure to 50 μmol m^{-2}s^{-1} for 10 min in the presence of DCMU (10 μM); downwards triangles, *dum22* cells; upwards triangles, *dum22 stt7–9* cells. (*D*) PSI antenna size as evaluated form the light saturation curve for P$_{700}$ oxidation in intact cells. The curves were acquired by exposing the cells to flashes of laser light of varying intensity and measuring the resulting P$_{700}$ oxidation. Traces were measured in the presence of hydroxylamine (1 mM) and DCMU (20 μM) to prevent PSII charge separation. Symbols are as in *B*.

to either state 1 or state 2 (20). To test possible changes in the reaction center (RC) stoichiometry in *dum22* cells, which are acclimated to state 2 (18), and in *stt7–9* and *dum22 stt7–9* cells, which are, in principle, locked in state 1 (5), we used a spectroscopic approach based on the amplitude of the light-induced electrochromic shift (ECS). This technique has been used successfully to evaluate the PSI/PSII stoichiometry in freshwater green algae (21). As shown in Fig. 2*A*, very minor differences were seen between the different strains, suggesting that the absence of ST has no significant effect on the RC stoichiometry, at least in *Chlamydomonas* (1).

We next assessed the balance in light energy distribution between the 2 photosystems that should be affected by the inability of *stt7–9* and of *dum22 stt7–9* to perform ST. We first evaluated the PSII antenna in cells that were dark-adapted for $\approx$30 min after being grown photoautotrophically in low light (i.e., conditions in which the growth phenotype of *dum22 stt7–9* cells is maximum). To this aim, we measured the rate of chlorophyll fluorescence induction from open (F$_0$) to closed (F$_m$) PSII centers in the presence of 3-(3′,4′-dichlorophenyl)-1,1-dimethylurea (DCMU). This parameter, which is related quantitatively to the absorption cross-section of this photosystem (22) was 2 times slower in *dum22* (Fig. 2*B*) than in *dum22 stt7–9*, *stt7–9*, and wild-type cells. In addition, illumination of *dum22* in the presence of DCMU for 10 min (a treatment known to promote transition to state 1 via oxidation of the PQ pool) (17, 18) increased its rate of fluorescence induction to values close to those measured in the other strains, but such treatment had no effect on *dum22 stt7–9* cells (Fig. 2*C*). Consistent with this finding, the ratio of PSI/PSII fluorescence emission at 77 K was higher in *dum22* cells than in the other strains in aerobic

conditions, but it decreased to similar values when illuminated in the presence of DCMU (Table S1). Together, these data confirm that the dum22 stt9–7 mutant was mostly in a state 1 condition, because it lacked the Stt7 kinase, whereas the *dum22* mutant was in state 2. We next assessed changes in PSI antennae by measuring the light saturation curve for oxidation of the primary electron donor of PSI (P_{700}) (23). Dark-adapted cells placed in aerobic conditions were exposed to a laser flash (duration 5 ns) of variable intensity, and the light-induced oxidation of P_{700} was estimated from the amplitude of the 4-μs component of the decay-associated spectra of P_{700}^+ (24). As shown in Fig. 2D, a larger P_{700} oxidation was observed in *dum22* cells upon excitation with limiting light intensities. In agreement with previous functional (13) and biochemical (14) studies in wild-type cells, this increased P_{700} oxidation indicates that the 2-fold decrease in PSII absorption capacity caused by state 2 acclimation is accompanied by a similar increase in the PSI antenna size.

Increasing the PSI absorption capacity at the expense of PSII, as observed in *dum22*, should lead to unbalanced excitation of the 2 photosystems at limiting photon flux. To evaluate this possibility, we measured the redox state of P_{700} in steady-state continuous illumination. Again, experiments were conducted in conditions in which growth was affected mostly in the *dum22 stt7–9* mutant, i.e., photoautotrophic growth in low light. Furthermore, we added an artificial PSI electron acceptor, methyl viologen (MV, 2 mM), to avoid any kinetic limitation by the PSI acceptor side and/or to avoid accumulation of reduced ferredoxin and NADPH, which may lead to re-injection of electrons into the intersystem electron carriers through CEF (25). Fig. 3A shows typical kinetics of P_{700} oxidation in wild-type, *stt7–9*, *dum22*, and *dum22 stt7–9* using continuous illumination of limiting intensity (50 μmol photons m^{-2}s^{-1}) or saturating intensity (800 μmol photons m^{-2}s^{-1}). These traces were used to estimate the light-saturation profiles of P_{700} oxidation in the 4 strains. As shown by the large difference in these profiles (Fig. 3B), photon absorption was unbalanced in favor of PSI in *dum22* cells when compared to the 3 other strains, consistent with the transfer of light-harvesting antenna from PSII to PSI. Addition of the PSII inhibitor DCMU to MV-treated cells largely enhanced P_{700} oxidation (Fig. S3), confirming that most of the electrons delivered to P_{700}^+ were of PSII origin. However, in the presence of both chemicals we noted an incomplete oxidation of P_{700} at low light intensities in all strains. We tentatively attribute this DCMU-insensitive electron pathway to the NADPH dehydrogenase (NDH)-mediated chlororespiratory pathway (26, 17). Using the same procedure used to evaluate the rate of electron flow in DCMU-poised cells (see Table 1), we evaluated the maximum electron flow capacity of this pathway to be ≈2 to 3 electrons/PSI/s in wild-type cells.

Light-Dependent Plus Enhanced Light-Independent Plastoquinone Reduction Decreases Photosynthetic Yield at Low Light in *dum22 stt7–9*. We next tested the overall photosynthetic activity by measuring oxygen evolution and fluorescence changes at different light intensities in wild-type, *stt7–9*, *dum22*, and *dum22 stt7–9* cells in photoautotrophic conditions. In all strains, very similar maximum oxygen evolution rates were observed (Fig. 3C). However, a drastic inhibition of photosynthesis (65% to 75%) appeared in *dum22 stt7–9* cells at limiting light intensities, whereas photosynthesis decreased by only ≈35% in *dum22* when compared with wild-type and *stt7–9* cells (Fig. 3C, *Inset*). The reduced photosynthetic activity in *dum22 stt7–9* cells also was accompanied by a drop in the quantum yield of linear electron flow as measured by the fluorescence parameter ΦPSII (Fig. 3D) (27). This experiment reveals that, in *Chlamydomonas*, efficient photosynthesis cannot take place in an ST-impaired mutant when respiration is inhibited. However, the mere inhibition of ST is insufficient to modify photosynthesis when the stromal redox
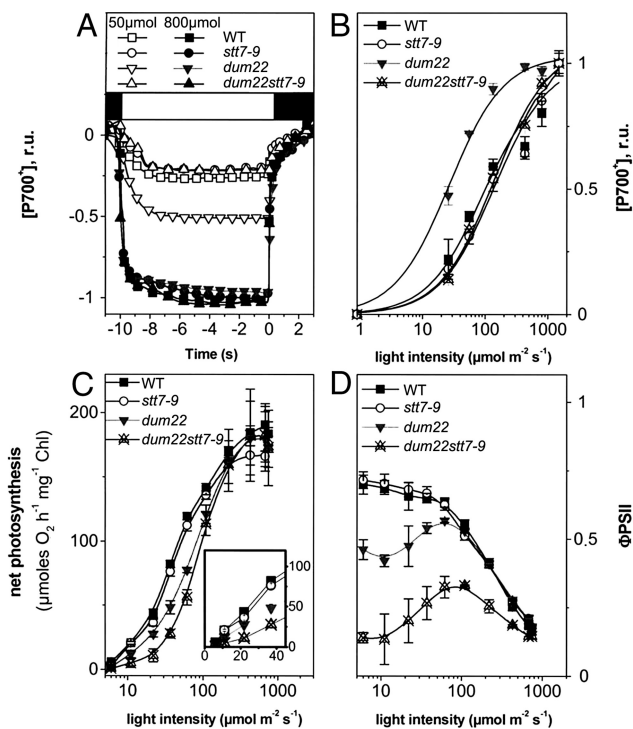
Fig. 3. Electron transfer reactions in continuous light. (*A*) P_{700} oxidation kinetics measured in continuous light in the presence of MV (2 mM). Open symbols, 50 μmol m^{-2}s^{-1}; solid symbols, 800 μmol m^{-2}s^{-1}; black square, actinic light off; white square, actinic light on. (*B*) Light saturation of P_{700} oxidation evaluated from data as in *A*. The time at which the light was switched off is considered time 0. Black squares, wild-type cells; open circles, *stt7–9* cells; downwards gray triangles, *dum22* cells; upwards crossed triangles, *dum22 stt7–9* mutant cells. (*C*) Light saturation curves of oxygen evolution in wild-type cells (*black squares*), *stt7–9* cells (*open circles*), *dum22* cells (*black downwards triangles*), and *dum22 stt7–9* mutant cells (*upwards crossed triangles*). Photosynthetic activity was calculated as "net photosynthesis" (i.e., photosynthesis after correction for respiration) at any given light intensity. (*D*) ΦPSII, calculated as (*Fm*−*Fs*)/*Fm*. Error bars indicate standard error of the mean of 3 independent measurements.

pressure is low, because of sustained respiratory activity, as shown by the lack of phenotype in *stt7–9* cells. Thus, the rationale for the inhibition observed in *dum22 stt7–9* cells should be found in 2 processes that develop with changes in the redox poise of the stromal compartment when respiration is inhibited. First, both the *dum22* cells and *dum22 stt7–9* mutants display a high level of non-photochemical reduction of the PQ pool because of the Pasteur effect associated with their respiratory defect (see introduction). This large electron reservoir for PSI turnover is paralleled by a higher PSI light-harvesting capacity only in *dum22* cells, because they undergo a transition to state 2; the *dum22 stt7–9* mutant, in contrast, is locked in state 1 and keeps a small PSI antenna. It therefore seems that the rate of PSI-driven oxidation of the PQ pool in the *dum22 stt7–9* mutant cannot cope with the rate of PSII-driven photochemical reduction combined with enhanced rates of stromal-driven non-photochemical reduction; as a result, reducing equivalents accumulate among the intersystem electron carriers (Fig. 3 *B* and *D*), and overall photosynthetic activity (Fig. 3C) and biomass production decrease. Still, the enhanced reduction pressure from the stroma would be expected to enhance CEF (25). However, the impaired transition to state 2 in *dum22 stt7–9* mutants should lead to a diminished CEF in light-limiting conditions because the PSI antenna are smaller in *dum22 stt7–9* mutants than in *dum22* cells To test this hypothesis, we assessed the efficiency of CEF

Table 1. Relative cyclic electron flow (CEF) and cellular ATP content in wild-type, *stt7–9*, *dum22*, and *dum22 stt7–9* cells

Strain	CEF	ATP TAP Dark	ATP TAP hν	ATP Min hν
Wild type	0.35 ± 0.05	66.2 ± 6.8	100	93.0 ± 9.1
stt7–9	0.37 ± 0.05	55.9 ± 6.1	102.3 ± 12.3	83.8 ± 20.4
dum22	0.63 ± 0.09	3.0 ± 1.3	69.0 ± 10.0	69.0 ± 10.0
dum22 stt7–9	0.35 ± 0.02	1.8 ± 2.1	65.7 ± 6.5	71.2 ± 2.7

CEF was evaluated as $= k * [P_{700}^+]/([P_{700}^+]+[P_{700}])$ after illumination in the presence of DCMU (20 μM), where k represents the P_{700}^+ re-reduction rate after steady-state illumination of saturating intensity. CEF rates at low light (50 μmol m^{-2} s^{-1}) are normalized to the maximum value (typically 12.5 ± 0.1 s^{-1} in wild-type cells). Standard deviation is relative to at least 5 replicates. ATP is expressed in percentage of the wild-type control (107 ± 12 nmol/mg Chlorophyll-1). Cells were fixed after 3 h in the dark or after continuous illumination with low light (50 μmol m^{-2}s^{-1}).

by measuring the redox changes of P_{700} (using the approach in Fig. 3*A*) in the presence of the sole PSII inhibitor DCMU. When PSII activity is prevented, the rate of P_{700} re reduction after illumination allows the rate of CEF to be determined (28). The flow rate of this process (i.e., the number of electrons transferred per PSI per unit of time) was evaluated as $k * [P_{700}^+]/([P_{700}^+]+[P_{700}])$, where k is the P_{700}^+ reduction rate after full oxidation by 10 s of saturating light and $[P_{700}^+]/([P_{700}^+]+[P_{700}])$ is the oxidation level at any light intensity. Table 1 shows that although the relative efficiency of CEF decreased at low light (50 μmol m^{-2} s^{-1}) in all strains, the CEF rate was much higher in *dum22* cells that were locked in state 2 than in the other strains that remained in state 1.

Because CEF should contribute significantly to ATP synthesis upon illumination, we compared the steady-state cellular ATP levels. Table 1 shows that, despite changes in CEF and the overall photosynthetic activity, no differences in ATP levels were seen between *dum22* cells and *dum22 stt7–9* mutant cells in either mixotrophic or photoautotrophic conditions in the light. As expected, because of their respiratory deficiencies, the 2 strains showed ATP depletion upon dark incubation and a slightly lower ATP content in the light than seen in their wild-type and *stt7–9* counterparts.

Discussion

In plants, ST is regarded as a regulatory process of photosynthesis that optimizes linear electron flow by a proper balance of energy distribution between the 2 photosystems (3). In microalgae such as *Chlamydomonas*, STs have been proposed to tune the ratio of CEF to linear electron flow in photosynthesis in response to changes in the intracellular demand for ATP (2). It therefore was somewhat paradoxical that the absence of ST in a phototrophic mutant of *Chlamydomonas* lacking the Stt7 kinase had no effect on its growth characteristics when compared with the wild type (ref. 16 and the present study). This lack of growth phenotype can be understood better if the energy contribution of the mitochondria (the major cellular energy producer besides the chloroplast) is taken into account. In algae, the tight metabolic interaction between the 2 bioenergetic compartments is exemplified by the modulation of the redox poise of the PQ pool in the thylakoid membranes by the efficiency of respiration (18). In another instance, a second site-suppressor mutant of a chloroplast ATP synthase mutant of *Chlamydomonas* (Fud50) (29), which still was devoid of the chloroplast enzyme, could grow photoautotrophically, unlike the original mutant strain. In this new genetic context, ATP exchange between the mitochondrion and the chloroplast became efficient enough to provide all the ATP required for photosynthetic CO_2 assimilation in vivo.

Here we show that the ability to perform ST becomes critical for phototrophic growth in a respiration-deficient context. The double mutant *dum22 stt7–9*, lacking the Stt7 kinase and defective for respiration, is locked in state 1, i.e., in conditions in which the absorption properties of both photosystems are similar (13). Although this condition should be ideally suited for electron flow from water to CO_2, the *dum22 stt7–9* mutant grows more slowly than *dum22*, *stt7–9*, and wild-type strains in photoautotrophic conditions under limiting white-light conditions. This observation can be explained as follows. Non-photochemical reduction of the PQ pool by the thylakoid-located NDH (26) is rather efficient in mitochondrial mutants of *Chlamydomonas*. Therefore, concomitant injection of electrons into the pool by photochemical (PSII) and non-photochemical (NDH) processes mimics an increase of PSII activity, which can be counterbalanced at low light only if PSI activity is enhanced. The massive increase in PSI absorption capacity (by a factor of ≈2) in *dum22* cells resulting from the constitutive acclimation to state 2 (Fig. 2) (18) highly favors PSI activity in low light, allowing reoxidation of the PQ pool and efficient utilization of light for biomass production. In contrast, more balanced light partitioning between PSII and PSI and over-reduction of the PQ pool in the *dum22 stt7–9* mutant, which is constitutively locked in state 1, becomes detrimental for light utilization at low photon density, as shown by its reduced photosynthetic performance in oxygen evolution and PSII efficiency, as derived from fluorescence emission (Fig. 3). Furthermore, the increased PSI sensitization in state 2 conditions, observed in the *dum22* mutant but not in the *dum22 stt7–9* mutant, should be accompanied by an enhanced CEF at low light around this complex (18). Indeed, the CEF rate was much lower in the *dum22 stt7–9* mutant than in *dum22* cells (Table 1). On the other hand, the Benson-Calvin cycle requires ATP and NADPH in a stoichiometry of 1.5, a ratio that cannot be fulfilled entirely by the sole operation of photosynthetic linear electron flow. Recent estimates suggest that this process has an insufficient proton-to-electron balance, when compared with the stoichiometry of H^+ required to fuel ATP synthesis by the chloroplast CF_o-F_i complex (30, 31). In *Chlamydomonas*, it can be estimated that no more than 1.4 ATP should be synthesized per NADPH (≈ 1.39) (15). Thus, even when light utilization is fully optimized, alternative processes must contribute to the generation of an "extra" ΔpH, i.e., of additional ATP synthesis to re-equilibrate the ATP/NADPH stoichiometry for proper carbon assimilation. Synthesis of ATP can be fueled by cyclic photophosphorylation, which does not require PSII activity (32), and also through the reduction of molecular oxygen by the Mehler reaction or the activity of plastid terminal oxidase (33). Mitochondria also can provide extra ATP while consuming reducing equivalents exported from the chloroplast via the malate or the triose phosphate transporter (34).

Our present study, which shows no differences in photosynthesis (Fig. 3) or growth (Fig. 1) between the wild-type cells and the *stt7–9* mutant impaired in ST, suggests that the mere inhibition of ST is not sufficient to impair biomass production by photosynthesis. Conversely, our results argue for a bioenergetic recruitment of mitochondria in relieving photosynthesis in the

absence of ST-driven CEF by providing extra ATP for photosynthesis. The bioenergetic contribution of mitochondria to photosynthesis-driven metabolism is exemplified by the lower intracellular ATP levels in photoautotrophic conditions under low light when respiration is blocked (in *dum22* cells), even if the PSI turnover and growth rate are not compromised. Of note, the ATP level reached upon exposure of *dum22* cells to low light is very close to that measured in the wild-type cells in the dark, suggesting that in low light photosynthesis in *dum22* cells still is capable of sustaining cell growth, although it is ATP limited. Thus, STs in the absence of respiration promote enough CEF-driven ATP synthesis for growth but place the cells in an ATP-limiting situation. Conversely, our observation that the ATP levels in *dum22 stt7–9* cells cannot be decreased further below the levels seen in *dum22* cells (Table 1) strongly suggests that below a threshold level, ATP becomes limiting for photosynthetic growth. This possibility is in agreement with previous data (35). Thus, the limited energy supply in the double mutant at low light probably is consumed in intracellular metabolism at the expense of biomass production and cell division. Ultimately, this limitation leads to a decrease in growth rate.

In conclusion, our study provides evidence for the contribution of the 2 major bioenergetic pathways to supply photosynthesis with the extra ATP required for carbon assimilation in *Chlamydomonas*. Oxidative phosphorylation in mitochondria seems to play a prominent role both in the dark-to-light transition, as previously proposed for vascular plants (36), and in steady-state, light-limited conditions. CEF, which is boosted in state 2 conditions, also contributes to this process and supplies ATP in the absence of energy supplied by mitochondria. The intimate relationship between the cellular respiratory capacity and the ability to modulate the PSI absorption cross-section through STs results in a tight interplay between CEF and respiration. This interplay seems to be particularly effective in *Chlamydomonas*. It provides these unicellular organisms with a very high photosynthetic flexibility in both ATP generation and electron transfer capacity in highly reducing conditions. This flexibility certainly is one of the major metabolic features enabling this alga to acclimate successfully to rapidly changing environmental conditions.

Materials and Methods

Strains and Growth Conditions. The *Chlamydomonas* wild-type strain used in this work is derived from the 137c strain (cc-1373 of the Duke University). The *Chlamydomonas dum22* strain is a deletion mutant lacking the left telomere, the *cob* gene, and part of the *nd4* gene (19). *Stt7–9* is a clone allelic to *stt7*, which can be crossed easily, unlike the original strain (gift from J.-D. Rochaix). The double mutant *dum22 stt7–9* was obtained by crossing the *dum22 mt$^-$* mutant with a *stt7–9 mt$^+$* mutant using standard procedures (see supplemental data for further information). We isolated 7 *dum22stt7–9* clones (Fig. S1) and further analyzed 2 of them (A1, J1,) for their photosynthetic features. Cells

were cultivated routinely at 50 μmol photons m^{-2}s^{-1} in mixotrophic (TAP) or photoautotrophic (Min) conditions.

Spectroscopy. Cells were harvested during exponential growth (2*10^6 cells/mL) and were resuspended at a concentration of 10^7 cells/mL^{-1} in minimum medium with the addition of 20% (wt/vol) Ficoll to prevent cell sedimentation. In vivo kinetics measurements were performed at room temperature with 2 different setups. Steady-state P$_{700}$ oxidation kinetics and RC stoichiometries were measured using a JTS spectrophotometer (Biologic, France). Continuous light was provided by a red source (630 nm), which was switched off transiently while measuring P$_{700}$ absorption changes at 705 nm. PSI and PSII content was estimated spectroscopically from changes in the amplitude of the fast phase (100 μs) of the ECS signal (at 520–545 nm) upon excitation with a saturating laser flash. The ECS spectral change linearly follows the number of light-induced charge separations within the reaction centers (37). Thus, the PSII contribution can be calculated from the decrease in the signal amplitude upon the addition of DCMU (20 μM) and hydroxylamine (1 mM) that irreversibly block PSII charge separation once the sample has been pre-illuminated (21). Conversely, PSI was estimated as the fraction of the signal that was insensitive to these inhibitors. The light-saturation profile of P$_{700}$ oxidation (Fig. 2*D*) was measured with a second setup with a time resolution of 10 ns. Actinic flashes were provided by a dye laser at 600 nm, the intensity of which was changed using neutral filters; detecting flashes were provided by an optical parametric oscillator. The extent of P$_{700}$ oxidation was evaluated from the 900 ns to 20 μs phase of absorption changes at 430 to 460 nm, in line with previously recorded spectra of the 4-μs component of the decay-associated spectra of P$_{700}^+$ in wild-type cells (24). Fluorescence inductions were measured using a home-built fluorometer. Excitation was provided by a green LED source (520 nm), and fluorescence was detected in the near IR region. PSII antenna size was evaluated by the rate of fluorescence induction in the presence of the PSII inhibitor DCMU. In the presence of this inhibitor, an average of 1 photon per PSII center is absorbed at time *t* (25). This parameter was estimated for every fluorescence induction trace to evaluate the number of absorbed photons. Fluorescence emission spectra at 77 K were recorded using a LS 50B spectrofluorometer (PerkinElmer). Excitation was at 440 nm, and emission was detected at 685 nm (PSII) and 715 nm (PSI). Spectra were corrected for the wavelength-dependent photomultiplier response.

Oxygen Evolution and ΦPSII. Oxygen evolution and the quantum yield of PSII in the light (ΦPSII) (27) were measured simultaneously using a Clark electrode connected to a modulated fluorometer (type MFMS, Hansatech Instruments) in Min liquid medium supplemented with 5 mM NaHCO$_3$. ΦPSII was calculated as (Fm′-Fs)/Fm′, where Fm′ is the maximum fluorescence emission level induced by a pulse of saturating light (≈5,000 μmol of photons m^{-2} s^{-1}), and Fs is the steady-state level of fluorescence emission. Chlorophyll concentration was adjusted to 5 μg/mL.

ATP Measurements. ATP was extracted as in (17) using 5% HClO$_4$. Samples were centrifuged at 10,000 × *g*, and a volume of the supernatant was diluted in 0.5 M Tris-Acetate, pH 7.75 (1/300, vol/vol). Determination of ATP content was made using the Enliten luciferase/luciferin kit (Promega) with a Lumat LB9501 apparatus (Berthold).

1. Rochaix JD (2007) Role of thylakoid protein kinases in photosynthetic acclimation. *FEBS Lett* 581:2768–2775.
2. Wollman FA (2001) State transitions reveal the dynamics and flexibility of the photosynthetic apparatus. *EMBO J* 20:3623–3630.
3. Allen JF (1992) How does protein phosphorylation regulate photosynthesis? *Trends Biochem Sci* 17:12–17.
4. Bellafiore S, Barneche F, Peltier G, Rochaix JD (2005) State transitions and light adaptation require chloroplast thylakoid protein kinase STN7. *Nature* 433:892–895.
5. Depege N, Bellafiore S, Rochaix JD (2003) Role of chloroplast protein kinase Stt7 in LHCII phosphorylation and state transition in *Chlamydomonas*. *Science* 299:1572–1575.
6. Gal A, Zer H, Ohad I (1997) Redox-controlled thylakoid protein phosphorylation: News and views. *Physiol Plant* 100:869–885.
7. Wollman FA, Lemaire C (1988) Studies on kinase-controlled state transitions in photosystem II and b$_6$f mutants from *Chlamydomonas reinhardtii* which lack quinone-binding proteins. *Biochim Biophys Acta* 85:85–94.
8. Allen J (2002) Photosynthesis of ATP-electrons, proton pumps, rotors, and poise. *Cell* 110:273–276.
9. Tikkanen M, et al. (2006) State transitions revisited—a buffering system for dynamic low light acclimation of *Arabidopsis*. *Plant Mol Biol* 62:779–793.
10. Bonardi V, et al. (2005) Photosystem II core phosphorylation and photosynthetic acclimation require two different protein kinases. *Nature* 437:1179–1182.
11. Lunde C, Jensen PE, Haldrup A, Knoetzel J, Scheller HV (2000) The PSI-H subunit of photosystem I is essential for state transitions in plant photosynthesis. *Nature* 408:613–615.
12. Frenkel M, Bellafiore S, Rochaix JD, Jansson S (2007) Hierarchy amongst photosynthetic acclimation responses for plant fitness. *Physiol Plant* 129:455–459.
13. Delosme R, Olive J, Wollman FA (1996) Changes in light energy distribution upon state transitions: An in vivo photoacoustic study of the wild-type and photosynthesis mutants from *Chlamydomonas reinhardtii*. *Biochim Biophys Acta* 1273:150–158.
14. Takahashi H, Iwai M, Takahashi Y, Minagawa J (2006) Identification of the mobile light-harvesting complex II polypeptides for state transitions in *Chlamydomonas reinhardtii*. *Proc Natl Acad Sci USA* 103:477–482.
15. Eberhardt S, Finazzi G, Wollman FA (2008) The dynamics of photosynthesis. *Annu Rev Genet* 42:463–515.
16. Fleischmann MM, et al. (1999) Isolation and characterization of photoautotrophic mutants of *Chlamydomonas reinhardtii* deficient in state transition. *J Biol Chem* 274:30987–30994.
17. Bulté L, Gans P, Rebeillé F, Wollman FA (1990) ATP control on state transitions in vivo in *Chlamydomonas reinhardtii*. *Biochim Biophys Acta* 1020:72–80.

PLANT BIOLOGY

18. Cardol P, et al. (2003) Photosynthesis and state transitions in mitochondrial mutants of *Chlamydomonas reinhardtii* affected in respiration. *Plant Physiol* 133:2010–2020.
19. Cardol P, Remacle C (2008) in *The Chlamydomonas Source Book 3*, eds. Stern D, Harris EE (Elsevier, Amsterdam) Vol. 2, Organellar and Metabolic Processes.
20. Dietzel L, Brautigam K, Pfannschmidt T (2008) Photosynthetic acclimation: State transitions and adjustment of photosystem stoichiometry—functional relationships between short-term and long-term light quality acclimation in plants. *FEBS Journal* 275:1080–1088.
21. Joliot P, Delosme R (1974) Flash-induced 519 nm absorption change in green algae. *Biochim Biophys Acta* 357:267–284.
22. Butler WL (1978) Energy distribution in the photochemical apparatus of photosynthesis. *Annu Rev Plant Physiol* 29:345–378.
23. Samson G, Bruce D (1995) Complementary changes in absorption cross-sections of Photosystems I and II due to phosphorylation and Mg2+-depletion in spinach thylakoids. *Biochim Biophys Acta* 1232:21–26.
24. Finazzi G, Sommer F, Hippler M (2005) Release of oxidized plastocyanin from photosystem I and cytochrome b6f complex in vivo. *Proc Natl Acad Sci USA* 102:7031–7036.
25. Joliot P, Joliot A (2006) Cyclic electron flow in C3 plants. *Biochim Biophys Acta* 1757:362–368.
26. Jans F, et al. (2008) A type II NAD(P)H dehydrogenase mediates light-independent plastoquinone reduction in the chloroplast of *Chlamydomonas. Proc Natl Acad Sci USA* 105:20546–20551.
27. Genty B, Harbinson J, Briantais J-M, Baker NR (1990) The relationship between non-photochemical quenching of chlorophyll fluorescence and the rate of photosystem 2 photochemistry in leaves. *Photosynth Res* 25:249–257.

28. Maxwell PC, Biggins J (1976) Role of cyclic electron transport in photosynthesis as measured by the photoinduced turnover of P700 in vivo. *Biochemistry* 15:3975–3981.
29. Lemaire C, Wollman FA, Bennoun P (1988) Restoration of phototrophic growth in a mutant of *Chlamydomonas reinhardtii* in which the chloroplast *atpB* gene of the ATP synthase has a deletion: An example of mitochondria-dependent photosynthesis. *Proc Natl Acad Sci USA* 85:1344–1348.
30. Allen JF (2003) Cyclic, pseudocyclic and noncyclic photophosphorylation: New links in the chain. *Trends in Plant Science* 8:15–19.
31. Steigmiller S, Turina P, Graber P (2008) The thermodynamic H+/ATP ratios of the H+-ATPsynthases from chloroplasts and *Escherichia coli. Proc Natl Acad Sci USA* 105:3745–3750.
32. Arnon DI (1959) Conversion of light into chemical energy in photosynthesis. *Nature* 184:10–21.
33. Ort DR, Baker NR (2002) A photoprotective role for O(2) as an alternative electron sink in photosynthesis? *Current Opinion in Plant Biology* 5:193–198.
34. Noguchi K, Yoshida K (2008) Interaction between photosynthesis and respiration in illuminated leaves. *Mitochondrion* 8:87–99.
35. Forti G, Furia A, Bombelli P, Finazzi G (2003) In vivo changes of the oxidation-reduction state of NADP and of the ATP/ADP cellular ratio linked to the photosynthetic activity in *Chlamydomonas reinhardtii. Plant Physiol* 132:1464–1474.
36. Dutilleul C, et al. (2003) Functional mitochondrial complex I is required by tobacco leaves for optimal photosynthetic performance in photorespiratory conditions and during transients. *Plant Physiol* 131:264–275.
37. Witt HT (1979) Energy conversion in the functional membrane of photosynthesis. Analysis by light pulse and electric pulse methods. The central role of the electric field. *Biochim Biophys Acta* 505:355–427.